mispairs with significant glycosyl bond dihedral angle deviations from those of the standard Watson-Crick pairs.[2a] Therefore, base mispairs are much more likely to contain unfavored tautomers that allow glycosyl bond geometry very close to that of the standard Watson-Crick pairs, i.e., A amino·C imino/keto,[2a] A imino·C amino/keto,[2a] or A amino·$C^+$ im/imol$H^+$ (Figure 12c). Hence, what is observed at equilibrium need not be what gives rise to the initial mispairing event.

## Conclusions

A minor tautomer of protonated cytidine has a population in aqueous solution possibly in the range of 10-30%, which is detectable by UVRR spectroscopy via its distinctive 1730-$cm^{-1}$ band. On the basis of comparisons with model compounds, the frequency and $D_2O$ sensitivity of this band identify the tautomer as the structure with an iminol bond and a protonated exocyclic imine. Tautomerization is suppressed in hemiprotonated poly($C^+$·C) by the H-bonding constraints of the $C^+$·C base pair in the duplex structure. The reappearance of the tautomer band at low pH indicates that fully protonated poly($C^+$·$C^+$) does not form a base-paired duplex. The iminol tautomer of $C^+$ may be an important contributor to the observed wobble pairing of A-C oppositions in duplex structures.

**Acknowledgment.** This work was supported by National Institutes of Health Grants GM 25158 (to T.G.S.) and GM 42936 (to J.R.F.) and by National Science Foundation Grant DMB 8419060 (to J.R.F.).

# X-ray Absorption Spectroscopic Studies of the Blue Copper Site: Metal and Ligand K-Edge Studies To Probe the Origin of the EPR Hyperfine Splitting in Plastocyanin

**Susan E. Shadle,[†] James E. Penner-Hahn,[§] Harvey J. Schugar,[⊥] Britt Hedman,*[,‡] Keith O. Hodgson,*[,†,‡] and Edward I. Solomon*[,†]**

*Contribution from the Department of Chemistry and Stanford Synchrotron Radiation Laboratory, Stanford University, Stanford, California 94305.* *Received June 15, 1992*

**Abstract:** X-ray absorption spectra for the oxidized blue copper protein plastocyanin and several Cu(II) model complexes have been measured at both the Cu K-edge and the ligand K-edges (Cl and S) in order to elucidate the source of the small parallel hyperfine splitting in the EPR spectra of blue copper centers. Assignment and analysis of a feature in the Cu K-edge X-ray absorption spectrum at ~8987 eV as the Cu 1s → 4p + ligand-to-metal charge-transfer shakedown transition has allowed for quantitation of 4p mixing into the ground-state wave function as reflected in the 1s → 3d (+4p) intensity at ~8979 eV. The results show that distorted tetrahedral ($D_{2d}$) $CuCl_4^{2-}$ is characterized by <4% Cu $4p_z$ mixing, while plastocyanin has only Cu $4p_{xy}$ mixing. Thus, the small parallel hyperfine splitting in the EPR spectra of $D_{2d}$ $CuCl_4^{2-}$ and of oxidized plastocyanin cannot be explained by 12% $4p_z$ mixing into the $3d_{x^2-y^2}$ orbital as had been previously postulated. Data collected at the Cl K-edge for $CuCl_4^{2-}$ show that the intensity of the ligand pre-edge feature at ~2820 eV reflects the degree of covalency between the metal half-occupied orbital and the ligands. The data show that $D_{2d}$ $CuCl_4^{2-}$ is not unusually covalent. The source of the small parallel splitting in the EPR of $D_{2d}$ $CuCl_4^{2-}$ is discussed. Experiments at the S K-edge (~2470 eV) show that plastocyanin is characterized by a highly covalent Cu-S(cysteine) bond relative to the cupric-thiolate model complex [Cu(tet *b*)(*o*-$SC_6H_4CO_2$)]·$H_2O$. Self-consistent-field-X$\alpha$-scattered-wave calculations have been used to understand copper-thiolate bonding in this model complex and to quantify the covalency reflected in the S K-edge intensity data. The XAS results demonstrate that the small parallel hyperfine splitting in the EPR spectra of blue copper sites reflects the high degree of covalency of the copper-thiolate bond.

## Introduction

The oxidized blue copper protein active site is characterized by unique spectral features compared to those of normal, tetragonal Cu(II) complexes.[1] The development of a detailed understanding of these features has been the goal of many experimental and theoretical studies. The intense blue color of the oxidized blue copper proteins results from an optical absorption at ~600 nm. The extinction coefficient of this feature is 2 orders of magnitude greater than that for absorption bands in the same region in normal tetragonal copper(II) complexes. Polarized absorption and low-temperature magnetic circular dichroism (MCD) studies in combination with self-consistent-field-X$\alpha$-scattered-wave (X$\alpha$) calculations have definitively assigned this feature as a S(Cys) $3p\pi \rightarrow$ Cu $3d_{x^2-y^2}$ charge-transfer (CT) transition.[2]

The EPR spectra of oxidized blue copper centers exhibit $g_\parallel > g_\perp > 2.00$, indicating that the half-occupied ground-state orbital is $3d_{x^2-y^2}$. The same ground state is found in normal tetragonal copper(II) complexes. However, the EPR spectra of blue copper centers exhibit unusually small parallel hyperfine splitting, the magnitude of which ($60 \times 10^{-4}$ $cm^{-1}$) is about one-third that of normal copper hyperfine splitting. The half-occupied 3d orbital associated with this EPR signal is involved in the electron-transfer reactivity of the blue copper center. Thus, to gain insight into the function of these proteins, it is essential to have a clear understanding of the electronic structural origin of the small $A_\parallel$ splitting associated with this ground-state wave function.

* Persons to whom correspondence should be addressed.
† Stanford University, Department of Chemistry.
‡ Stanford Synchrotron Radiation Laboratory.
§ Present address: Department of Chemistry, University of Michigan, Ann Arbor, MI 48109-1055.
⊥ Present address: Department of Chemistry, Rutgers University, The State University of New Jersey, New Brunswick, NJ 08903.

(1) (a) Solomon, E. I.; Penfield, K. W.; Wilcox, D. E. In *Structure and Bonding*; Hemmerich, P., et al., Eds.; Springer-Verlag: New York, 1983; pp 1-57. (b) Gray, H. B.; Solomon, E. I. In *Copper Proteins*; Spiro, T. G., Ed.; Wiley: New York, 1980; pp 1-39. (c) Adman, E. T. In *Advances in Protein Chemistry, Vol. 42, Metalloproteins: Structural Aspects*; Anfinsen, C. B., Edsall, J. T., Richards, F. M., Eisenberg, D. S., Eds.; Academic Press, Inc.: New York, 1991; pp 145-192.
(2) (a) Penfield, K. W.; Gewirth, A. A.; Solomon, E. I. *J. Am. Chem. Soc.* **1985**, *107*, 4519-4529. (b) Gewirth, A. A.; Solomon, E. I. *J. Am. Chem. Soc.* **1988**, *110*, 3811-3819.

0002-7863/93/1515-767$04.00/0 

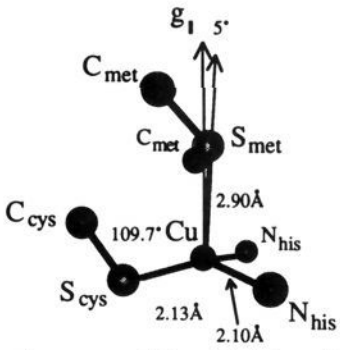


**Figure 1.** Active-site structure of the oxidized form of the blue copper protein plastocyanin. The copper is ligated in an effective $C_{3v}$ geometry by one cysteine, two histidines, and one methionine, which lies ~5° off the $g_\parallel$ direction.

Distorted tetrahedral ($D_{2d}$) $CuCl_4^{2-}$ exhibits small EPR parallel hyperfine splitting similar to that exhibited by blue copper centers (on the order of $<70 \times 10^{-4}$ cm$^{-1}$). One explanation for the reduced $A_\parallel$ splitting in distorted tetrahedral copper(II) complexes requires $4p_z$ mixing into the $3d_{x^2-y^2}$ ground-state wave function.[3] This mixing would reduce the hyperfine coupling because the $4p_z$ orbital has a spin dipolar contribution which opposes that of the $3d_{x^2-y^2}$ orbital, thus reducing the coupling between the unpaired electron spin and the copper nuclear spin. Sharnoff has calculated that for distorted tetrahedral ($D_{2d}$) $CuCl_4^{2-}$, 12% Cu $4p_z$ orbital character mixed into the half-occupied Cu 3d orbital would lower the hyperfine splitting value to the experimentally observed value.[4] Because spectroscopy[5] and subsequent crystal structures[6] of blue copper proteins have led to a description of the active site geometry as distorted tetrahedral, the reduced $A_\parallel$ splitting in the EPR of blue copper has also been explained by a $4p_z$ mixing mechanism.[7]

Single crystal EPR studies of plastocyanin, the most well characterized of the blue copper proteins, have shown that the unique axis ($g_\parallel$) is nearly aligned with the long Cu–thioether bond (Figure 1).[8] A ligand field analysis of the EPR data and of the near-IR ligand field transitions determined that the site is best described as having elongated $C_{3v}$ site symmetry with rhombic distortions.[8] In $C_{3v}$ symmetry, group theory allows the $3d_{x^2-y^2}$ orbital to mix with $4p_{xy}$, which would increase, not decrease, the $A_\parallel$ hyperfine splitting.

X$\alpha$ calculations have previously been performed on several copper(II) centers. In $D_{4h}$ $CuCl_4^{2-}$, which exhibits normal EPR hyperfine splitting, the ground-state wave function contains no 4p mixing due to inversion symmetry.[9] Calculations on the distorted tetrahedral ($D_{2d}$) $CuCl_4^{2-}$ complex indicate only ~4% $4p_z$ mixing into the ground-state $3d_{x^2-y^2}$ orbital.[9] Similar calculations on the plastocyanin site indicate that the protein site ground-state wave function contains only ~1% 4p mixing involving the $p_{xy}$ orbitals,[2] which is consistent with the $C_{3v}$ effective site symmetry described by the ligand field analysis. These results clearly question the possibility that 12% $4p_z$ mixing accounts for the small hyperfine in either the $D_{2d}$ complex or the blue copper site.

An alternative explanation for the small $A_\parallel$ hyperfine coupling constant of blue copper sites is unusually high covalency in the Cu–thiolate bond.[2] X$\alpha$ calculations indicate that the ground-state wave function is highly covalent, consisting of 42% Cu $3d_{x^2-y^2}$ and 36% S(Cys) 3p.[2] A high degree of covalency delocalizes the unpaired electron spin from the copper onto the cysteine ligand thereby reducing its coupling to the copper nuclear spin. Interestingly, the X$\alpha$ calculations on $D_{2d}$ $CuCl_4^{2-}$ do not indicate that its ground-state wave function is unusually covalent.[9]

Experimental studies of the magnitude and nature of Cu 4p mixing into the $3d_{x^2-y^2}$ ground state and of the covalency of these sites are necessary to determine the origin of the small hyperfine splitting in both the $D_{2d}$ $CuCl_4^{2-}$ and the blue copper centers. The results would thus provide important insight into the blue copper site, in particular into the electronic structure and copper–thiolate interaction of the ground-state wave function.

In order to evaluate $4p_z$ mixing, we have undertaken Cu K-edge X-ray absorption spectral (XAS) studies on $CuCl_4^{2-}$ complexes and the blue copper protein plastocyanin. The X-ray absorption near-edge structure, which contains transitions to bound states, is sensitive to the local electronic and geometric environment of the absorbing atom.[10] The electric dipole-allowed transition for any K-edge spectrum is 1s → np; mixing of np character into the final state of a forbidden transition causes the transition to have transition intensity. Previous K-edge studies of Cu(II) systems have observed a weak transition at ~8979 eV and a shoulder or partially resolved peak on the rising edge at ~8987 eV.[11] The peak at ~8979 eV is assigned as a 1s → 3d transition. In appropriate orientations, this transition has electric quadrupole-allowed intensity.[12] Further, as a formally forbidden electric dipole transition, it gains electric dipole intensity from 4p mixing into the half-occupied 3d orbital in appropriate site symmetries. As the electric dipole intensity of the 1s → 3d transition reflects the magnitude of 4p mixing into the half-occupied 3d orbital, these spectra serve as a probe of 4p mixing into the ground-state orbital. Polarized XAS studies of oriented single crystals provide a method for selecting and resolving the orientation dependence of near-edge features.[12-14] The high intensity and plane polarization of synchrotron radiation is ideal for performing these studies. Analysis of the polarized intensity of the 1s → 3d (~8979 eV) transition has previously enabled us to determine which Cu 4p orbital(s) contributes electric dipole intensity to the transition. Herein, we develop a protocol for quantitating this 4p mixing, which includes an analysis of the ~8987-eV feature.

As an experimental probe of the covalency of these sites, we have conducted XAS K-edge studies at the Cl and S K-edges. The K-edges of ligands like Cl and S fall in the 2–3-keV region where features are very well resolved.[15] Previously, we have shown

(3) Bates, C. A.; Moore, W. S.; Standley, K. J.; Stevens, K. W. H. *Proc. Phys. Soc.* **1962**, *79*, 73–83.
(4) Sharnoff, M. *J. Chem. Phys.* **1965**, *42*, 3383–3395.
(5) Solomon, E. I.; Hare, J. W.; Dooley, D. M.; Dawson, J. H.; Stephens, P. J.; Gray, H. B. *J. Am. Chem. Soc.* **1980**, *102*, 168–178.
(6) (a) Guss, J. M.; Freeman, H. C. *J. Mol. Biol.* **1983**, *169*, 521–563. (b) Adman, E. T.; Jensen, L. H. *Isr. J. Chem.* **1981**, *21*, 8–12.
(7) Roberts, J. E.; Brown, T. G.; Hoffman, B. M.; Peisach, J. *J. Am. Chem. Soc.* **1980**, *102*, 825–829.
(8) Penfield, K. W.; Gay, R. R.; Himmelwright, R. S.; Eickman, N. C.; Norris, V. A.; Freeman, H. C.; Solomon, E. I. *J. Am. Chem. Soc.* **1981**, *103*, 4382–4388.
(9) Gewirth, A. A.; Cohen, S. L.; Schugar, H. J.; Solomon, E. I. *Inorg. Chem.* **1987**, *26*, 1133–1146.
(10) (a) Srivastava, U. C.; Nigam, H. L. *Coord. Chem. Rev.* **1973**, *9*, 275–310, and references therein. (b) Agarwal, B. K.; Bhargava, C. B.; Vishnoi, A. N.; Seth, V. P. *J. Phys. Chem. Solids* **1976**, *37*, 725–728. (c) Kostroun, V. O.; Fairchild, R. W.; Kukkonen, C. A.; Wilkins, J. W. *Phys. Rev. B* **1976**, *13*, 3268–3271. (d) Schulman, R. G.; Yafet, Y.; Eisenberger, P.; Blumberg, W. E. *Proc. Natl. Acad. Sci. U.S.A.* **1976**, *73*, 1384–1388. (e) Belli, M.; Scafati, A.; Bianconi, A.; Mobilio, S.; Palladina, L.; Reale, A.; Burattini, E. *Solid State Commun.* **1980**, *35*, 355–361. (f) Kutzler, F. W.; Hodgson, K. O.; Doniach, S. *Phys. Rev. A* **1982**, *26*, 3020–3022. (g) Grunes, L. A. *Phys. Rev. B* **1983**, *27*, 2111–2131. (h) Sham, T. K. *J. Am. Chem. Soc.* **1983**, *105*, 2269–2273. (i) Cramer, S. P.; Eccles, T. K.; Kutzler, F. W.; Hodgson, K. O.; Mortenson, L. E. *J. Am. Chem. Soc.* **1976**, *98*, 1287–1288. (j) Horsley, J. A. *J. Chem. Phys.* **1982**, *76*, 1451–1458. (k) Bair, R. A.; Goddard, W. A., III *Phys. Rev. B* **1980**, *22*, 2767–2776.
(11) (a) Kau, L. S.; Spira-Solomon, D. J.; Penner-Hahn, J. E.; Hodgson, K. O.; Solomon, E. I. *J. Am. Chem. Soc.* **1987**, *109*, 6433–6442. (b) Smith, T. A.; Penner-Hahn, J. E.; Berding, M. A.; Doniach, S.; Hodgson, K. O. *J. Am. Chem. Soc.* **1985**, *107*, 5945–5955.
(12) Hahn, J. E.; Scott, R. A.; Hodgson, K. O.; Doniach, S.; Desjardins, S. R.; Solomon, E. I. *Chem. Phys. Lett.* **1982**, *88*, 595–598.
(13) Scott, R. A.; Hahn, J. E.; Doniach, S.; Freeman, H. C.; Hodgson, K. O. *J. Am. Chem. Soc.* **1982**, *104*, 5364–5369.
(14) (a) Hahn, J. E.; Hogdson, K. O. *ACS Symp. Ser.* **1983**, *211*, 431–444. (b) Templeton, D. H.; Templeton, L. K. *Acta Crystallogr., Sect. A* **1980**, *36*, 237–241. (c) Templeton, D. H.; Templeton, L. K. *Acta Crystallogr., Sect. A* **1982**, *38*, 62–67. (d) Heald, S. M.; Stern, E. A. *Phys. Rev. B* **1978**, *17*, 4069–4081. (e) Stern, E. A.; Sayers, D. E.; Lytle, F. W. *Phys. Rev. Lett.* **1976**, *37*, 298–301. (f) Stern, E. A.; Sayers, D. E.; Dash, J. G.; Shechter, H.; Bunker, B. *Phys. Rev. Lett.* **1977**, *38*, 767–770. (g) Cox, A. D.; Beaumont, J. H. *Philos. Mag. B* **1980**, *42*, 115–126. (h) Kutzler, F. W.; Scott, R. A.; Berg, J. M.; Hodgson, K. O.; Doniach, S.; Cramer, S. P.; Chang, C. H. *J. Am. Chem. Soc.* **1981**, *103*, 6083–6088.

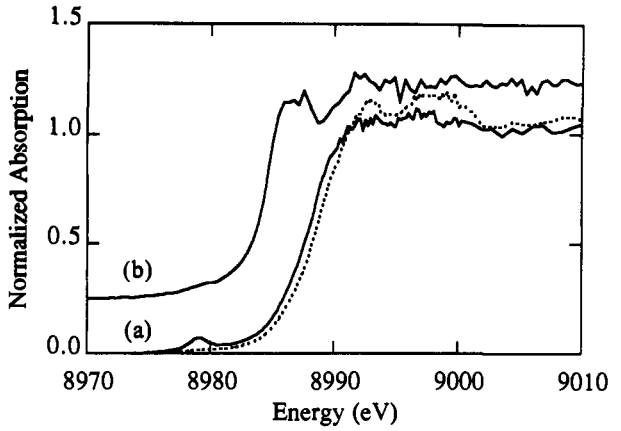


**Figure 2.** Polarized Cu K-edge spectra of $D_{4h}$ $CuCl_4^{2-}$. (a) *xy*-Polarized orientations for values of $\phi = 0°$ (---) and $\phi = 45°$ (—), where $\phi$ is collinear with the crystallographic *c* axis (taken from ref 12). The Cu 1s → 3d quadrupole transition intensity at ~8979 eV varies as $\sin^2(2\phi)$. (b) *z*-Polarized orientation (—). The prominent feature at ~8986 eV is assigned as the 1s → 4p + LMCT shakedown transition.

ligand K-edge XAS to be a useful probe of covalency in open-shell metal complexes.[16] In Cl K-edge studies of Cu(II)–Cl complexes, a sharp, intense pre-edge feature is observed at ~2820 eV and is assigned as a Cl 1s → Cu $3d_{x^2-y^2}$ transition, the half-occupied $3d_{x^2-y^2}$ orbital being the highest occupied molecular orbital. Due to the localized nature of the Cl 1s orbital, this transition can have absorption intensity only if the half-occupied 3d orbital contains a significant component of Cl 3p character as a result of covalency. Thus, a more accurate assignment of this transition is Cl 1s → $\psi^*$, where $\psi^* = (1 - \alpha'^2)^{1/2}(\text{Cu } 3d_{x^2-y^2}) - \alpha'(\text{Cl } 3p)$ and $\alpha'^2$ represents the amount of Cl 3p character in the antibonding orbital.[16] The electric dipole intensity for this transition is given by eq 1, which shows that the intensity observed in the pre-edge transition is simply the intensity of a 1s → 3p transition weighted by $\alpha'^2$. This approach allows us to experimentally probe ligand–metal covalency. It is particularly useful for sulfur ligands since naturally occurring isotopes of sulfur do not have a nuclear spin; thus experiments involving ligand superhyperfine are not accessible. We have measured the S K-edge X-ray absorption spectra of the model compound [Cu(tet *b*)($o$-$SC_6H_4CO_2$)]·$H_2O$ (Cu-tet *b*) and of the oxidized blue copper protein plastocyanin. Cu-tet *b* is ligated by a thiolate sulfur at 2.36 Å from the copper and four nitrogen ligands in a distorted 5-coordinate geometry. It has a $3d_{x^2-y^2}$ ground state[17] and exhibits normal EPR hyperfine splitting[18] and so provides a good comparison for the blue copper system. These studies at the S K-edge enable us to determine the degree of covalency between the copper and the cysteine sulfur in blue copper proteins. In order to quantitate the pre-edge intensity we have performed SCF-X$\alpha$-SW calculations on the Cu-tet *b* complex. X$\alpha$ calculations provide insight into the electronic structure and bonding of the system, in particular into the covalent character of the ground-state wave function.

$$I(\text{Cl 1s} \rightarrow \psi^*) = \alpha'^2 I(\text{Cl 1s} \rightarrow \text{Cl 3p}) \quad (1)$$

## Experimental Section

**A. Sample Preparation.** $(Creatininium)_2CuCl_4$[19] and $Cs_2CuCl_4$[4,20] were prepared according to published methods. Other details of the crystal preparation are as previously described in refs 12 and 21, respectively. The sample of [Cu(tet *b*)($o$-$SC_6H_4CO_2$)]·$H_2O$ was synthesized as described in the literature.[17] $Na_2S_2O_3 \cdot 5H_2O$ was purchased from J. T. Baker and used without further purification.

The purification and crystallization of poplar plastocyanin (*Populus nigra var italica*) used in the polarized Cu K-edge experiments has been described previously in the publication in which these spectra were ini-

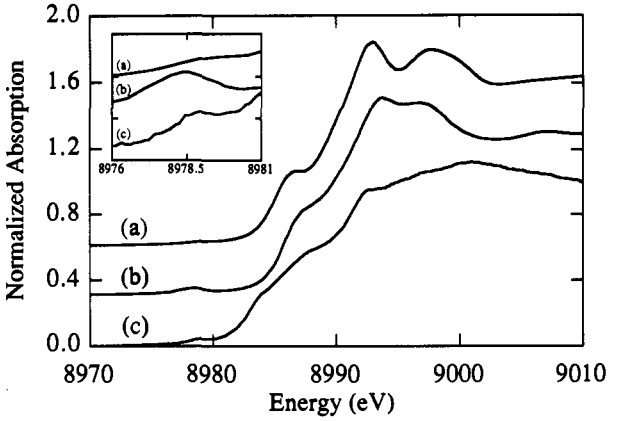


**Figure 3.** Nonpolarized (isotropic) Cu K-edge spectra of (a) $D_{4h}$ $CuCl_4^{2-}$, (b) $D_{2d}$ $CuCl_4^{2-}$, and (c) plastocyanin. Inset shows pre-edge region intensities multiplied by a factor of 5. The greater intensity in the 1s → 3d transition at ~8987 eV in both $D_{2d}$ $CuCl_4^{2-}$ and plastocyanin is due to 4p mixing into the ground-state orbital, giving the feature electric dipole-allowed intensity.

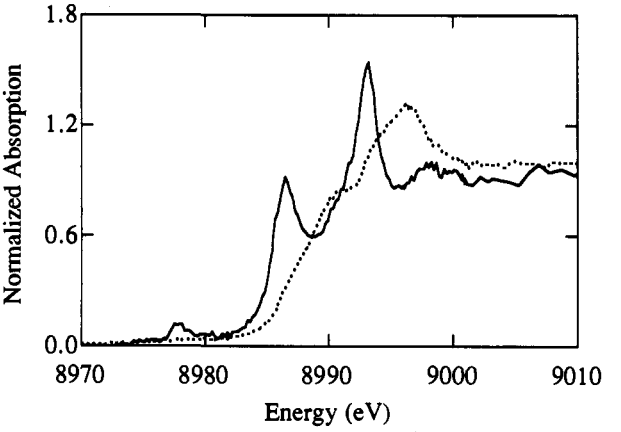


**Figure 4.** Polarized Cu K-edge spectra of $D_{2d}$ $CuCl_4^{2-}$. *z*-Polarized spectrum (—) and *y*-polarized spectrum (---). The feature in the *z*-polarized spectrum at ~8979 eV is assigned as the 1s → 3d (+$4p_z$) transition. The feature in the *z*-polarized spectrum ~8987 eV is assigned as the 1s → 4p + LMCT shakedown transition.

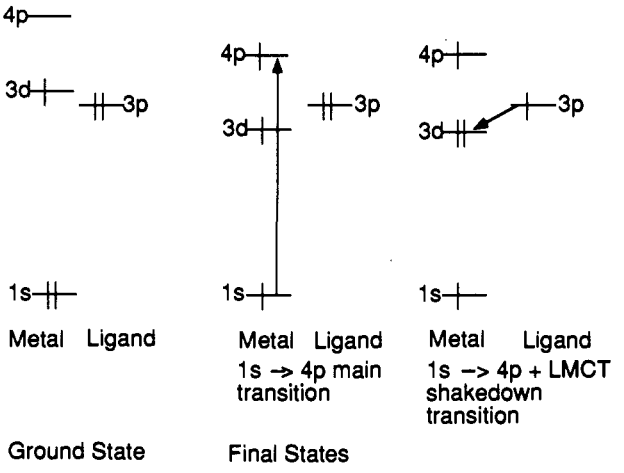


**Figure 5.** Schematic description of 1s → 4p Cu K-edge transition and its associated shakedown transition. Left: ground-state configuration. Center: excited 1s → 4p final state with relaxation of valence levels due to the creation of a core hole. Right: excited final state associated with the 1s → 4p + LMCT shakedown transition.

(15) The high-energy resolution is due to the combined effect of increased core-hole lifetime (Krause, M. O.; Oliver, J. H. *J. Phys. Chem. Ref. Data* **1979**, *8*, 329–338) and improved monochromator resolution.
(16) Hedman, B.; Hodgson, K. O.; Solomon, E. I. *J. Am. Chem. Soc.* **1990**, *112*, 1643–1645.
(17) Hughey, J. L., IV; Fawcett, T. G.; Rudich, S. M.; Lalancette, R. A.; Potenza, J. A.; Schugar, H. J. *J. Am. Chem. Soc.* **1979**, *101*, 2617–2623.
(18) Schugar, H. J., unpublished results.
(19) Udupa, M. R.; Krebs, B. *Inorg. Chim. Acta* **1979**, *33*, 241–244.
(20) McGinnety, J. A. *J. Am. Chem. Soc.* **1972**, *94*, 8406–8413.
(21) (a) Penner-Hahn, J. E. Ph.D. Thesis, Stanford University, 1984. (b) Smith, T. A. Ph.D. Thesis, Stanford University, 1985.

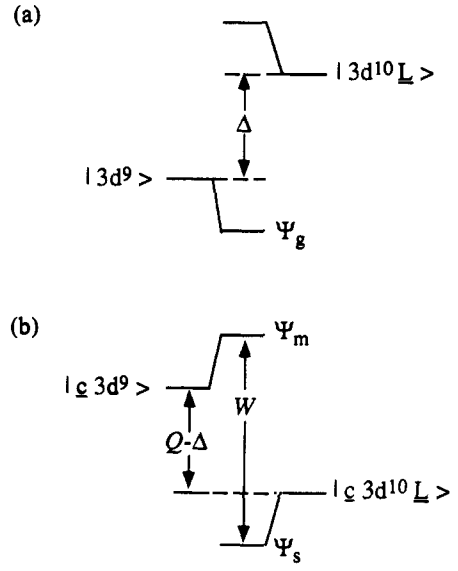


**Figure 6.** Configuration interaction formalism for analysis of the Cu K-edge near-edge structure. (a) Ground-state wave functions are determined by the parameters $T$ and $\Delta$. (b) Final-state wave functions. The lower-energy 1s → 4p + LMCT shakedown final state ($\Psi_s$) is separated in energy from the main 1s → 4p transition final state ($\Psi_m$) by the splitting $W$.

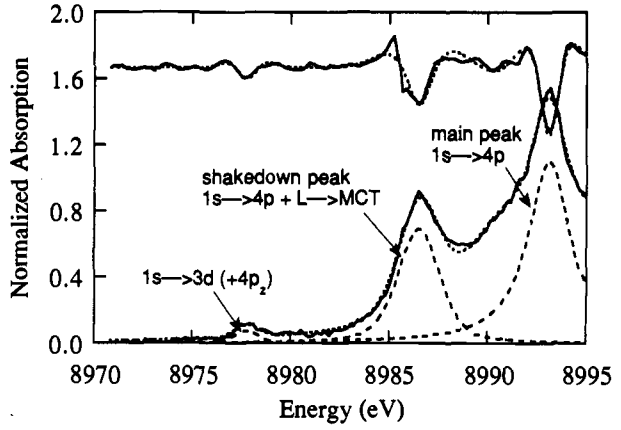


**Figure 7.** Representative fit to the data (bottom) and the second derivative (top) of $z$-polarized Cu K-edge spectra of $D_{2d}$ $CuCl_4^{2-}$. Fit is represented by a dashed line. Shown in the fit to the data are the functions used to model the 1s → 3d (+4$p_z$) transition at ~8979 eV, the 1s → 4p + LMCT transition at ~8987 eV, and the 1s → 4p main transition at ~8993 eV. The intensity of the main transition is not well established due to the rising-edge background.

tially reported.[13] Spectra shown in Figure 8 are data collected on crystal 7.[22] Plastocyanin used in the nonpolarized Cu K-edge experiments and in the S K-edge experiments was isolated from spinach chloroplasts according to published methods.[23]

For the Cu K-edge powder spectra, the metal complexes were ground into a fine powder and diluted in boron nitride. This mixture was then packed into an aluminum spacer sample holder and sealed with Mylar tape. For the ligand K-edge experiments, solid samples were ground into a fine powder which was thinly dispersed on Mylar tape (containing an acrylic adhesive determined to be free of chlorine and sulfur contaminants). The tape was mounted across the window of an aluminum plate.

Plastocyanin S K-edge protein measurements were made at room temperature. The protein solution (in 50 mM phosphate buffer, pH = 7.0) was preequilibrated in a buffer-saturated He atmosphere for ~1 h to minimize bubble formation in the sample cell. The protein solution was loaded via syringe into a 1-2-mm Teflon-brand cell sealed in back by a layer of Mylar tape and in front by a thin 6.4-$\mu$m polypropylene

(22) Note that the orientations shown in Figure 1 of ref 13 are those of crystal 2.

(23) Ellefson, W. L.; Ulrich, E. A.; Krogmann, D. W. In *Methods in Enzymology*; San Pietro, A., Ed.; McGraw-Hill: New York, 1980; pp 223-228; Vol. 69.

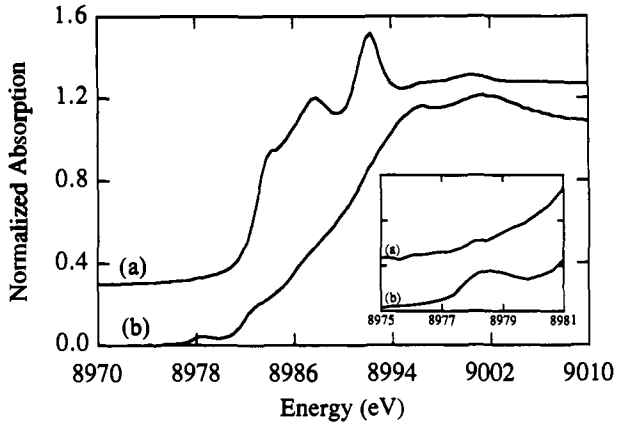


**Figure 8.** Polarized Cu K-edge spectra of poplar plastocyanin. (a) $z$-Polarized spectrum and (b) $xy$-polarized spectrum. Inset shows the expanded pre-edge region: the feature at ~8979 eV in the $xy$-polarized spectrum indicates that the plastocyanin ground state is characterized by $p_{xy}$ mixing. The absence of pre-edge intensity in the $z$-polarized spectrum reveals that there is no $p_z$ mixing (data are taken from ref 13).

window. UV-vis spectroscopy was used to verify the integrity of the sample both before and after exposure to the X-ray beam.

**B. Crystal Alignment.** $(Creatininium)_2CuCl_4$,[19] $Cs_2CuCl_4$,[20] and poplar plastocyanin[6a] have been structurally characterized by X-ray diffraction. The molecular site symmetry of $(creatininium)_2CuCl_4$ is approximately $D_{4h}$. The site symmetry of $Cs_2CuCl_4$ will be discussed later in this section. The published atomic coordinates were used to determine the orientation of specific molecular directions relative to the crystal axes. Integer $hkl$ values corresponding to a set of lattice planes perpendicular to the chosen molecular directions were then calculated with use of the known unit cell parameters. The alignment procedure finds the $\phi$ and $\chi$ values which place the desired molecular orientation perpendicular to the incoming radiation and in the horizontal plane. Since synchrotron radiation is highly polarized in the horizontal plane, the alignment provides for orientation of the molecular vector of interest to be parallel to the electric vector (**E**) of the incoming radiation. Specific crystal alignment and crystal positioning procedures for $(creatinium)_2CuCl_4$,[12] $Cs_2CuCl_4$,[21] and poplar plastocyanin[13] are described in earlier publications of these spectra.

**C. X-ray Absorption Measurements and Data Acquisition.** All data were collected at the Stanford Synchrotron Radiation Laboratory under dedicated operation (3.0 GeV, ~50 mA) with the SPEAR storage ring.

(i) **Cu K-Edges.** $(Creatininium)_2CuCl_4$ and plastocyanin polarized Cu K-edge data were collected on beam line 2-2; experimental details are described in refs 12 and 13, respectively. $Cs_2CuCl_4$ polarized Cu K-edge data were collected in fluorescence mode on beam line 4-2; experimental details are described in ref 21. Nonpolarized data of $(creatinium)_2CuCl_4$ and $Cs_2CuCl_4$ were measured in transmission mode at room temperature on beam line 2-2. Plastocyanin solution data were collected in fluorescence mode at 35 K using a Ge 13-element array detector on beam line 7-3.

A Si(220) double-crystal monochromator was utilized for energy selection for all Cu K-edge measurements. The monochromator was detuned 50% to minimize higher harmonic components in the X-ray beam. Data for the above samples were measured from ~8970 to ~9300 eV, with a step size of ~0.2 eV in the edge region (8970-9050 eV). For the Cu K-edge experiments, a third ion chamber was used for internal calibration by the simultaneous measurement of the absorption of a Cu foil placed between the second and third ion chambers. The first inflection point of the Cu foil edge spectrum was assigned to 8980.3 eV.

(ii) **Sulfur K-Edges.** Sulfur K-edge data were measured using the 54-pole wiggler beam line 6-2 in low magnetic field mode (5 kG) with a Pt-coated focusing mirror and a Si(111) double-crystal monochromator. The monochromator was detuned ~30% to minimize higher harmonic components in the X-ray beam. Details of the optimization of this beamline for low-energy studies and the experimental setup have been given in an earlier publication.[24]

The data were collected as fluorescence excitation spectra.[24] The energy was calibrated from the S K-edge spectra of $Na_2S_2O_3 \cdot 5H_2O$, run at intervals between the sample scans. The maximum of the first pre-edge feature in this spectrum was assigned to 2472.02 eV. Data were

(24) Hedman, B.; Frank, P.; Gheller, S. F.; Roe, A. L.; Newton, W. E.; Hodgson, K. O. *J. Am. Chem. Soc.* **1988**, *110*, 3798-3804.

**Table I.** Nonlinear Least-Squares Fits of *z*-Polarized Cu K-Edge XAS Spectrum of $D_{2d}$ $CuCl_4^{2-}$ [a,b]

| | | peak 1[c] (Gaussian) | peak 2[d] (Gaussian/Lorentzian) | peak 3[e] (Lorentzian) | peak 4[f] (Lorentzian) | ratio: peak 1/peak 2 |
|---|---|---|---|---|---|---|
| fit A | Ht | 0.075642 | 0.39879/0.29177 | 0.49692 | 1.0991 | |
| | FWHM | 1.4768 | 2.454/2.6102 | 4.8 | 2.5763 | 0.0642 |
| | center | 8977.8 | 8986.5 | 8990.5 | 8993.1 | |
| fit B | Ht | 0.075936 | 0.39137/0.30306 | 0.49392 | 1.1042 | |
| | FWHM | 1.4796 | 2.4643/2.6306 | 4.7 | 2.5830 | 0.0639 |
| | center | 8977.8 | 8986.5 | 8990.5 | 8993.1 | |
| fit C | Ht | 0.076211 | 0.38398/0.31429 | 0.49086 | 1.1094 | |
| | FWHM | 1.4821 | 2.4751/2.63296 | 4.6 | 2.5899 | 0.0636 |
| | center | 8977.8 | 8986.5 | 8990.5 | 8993.1 | |
| fit D | Ht | 0.076464 | 0.37663/0.32540 | 0.48772 | 1.1145 | |
| | FWHM | 1.4845 | 2.487/2.6372 | 4.5 | 2.5971 | 0.0632 |
| | center | 8977.8 | 8986.5 | 8990.5 | 8993.1 | |
| fit E | Ht | 0.076692 | 0.36935/0.33636 | 0.48449 | 1.1195 | |
| | FWHM | 1.4866 | 2.5003/2.6433 | 4.4 | 2.6044 | 0.0629 |
| | center | 8977.8 | 8986.5 | 8990.4 | 8993.1 | |
| average peak area | | 0.1129 | 1.7764 | | 2.8734 | 0.0636 |
| standard deviation | | 0.0009 | 0.0287 | | 0.0333 | 0.000514 |

[a] Underlined values indicate that the parameter was fixed during this fit. [b] An additional Lorentzian function (not shown) was used to model the rising-edge background. [c] Peak 1 models the 1s → 3d transition at ~8979 eV. [d] Peak 2 models the 1s → 4p + LMCT shakedown transition at ~8987 eV. [e] Peak 3 was required to reproduce the data and the second derivative of the data. [f] Peak 4 models the 1s → 4p main transition 6.6 eV above the shakedown transition.

collected from 2420 to 2740 eV, with a step size of 0.08 eV in the edge region. The spectrometer resolution was ~0.5 eV.[24] A reproducibility in edge position determination better than 0.2 eV for these experiments was obtained by calculating and comparing first and second derivatives for model compounds measured during different experimental sessions.

**D. Data Analysis.** A smooth pre-edge background was removed from all spectra by fitting a polynomial to the pre-edge region and subtracting this polynomial from the entire spectrum. Normalization of the data was accomplished by fitting a flat polynomial or a straight line to the post-edge region and normalizing the edge jump to 1.0 at 9000 eV for the copper edges and at 2490 eV for the sulfur edges.

**Analysis of Polarized Data.** Description of the crystallographic systems in $(creatininium)_2CuCl_4$[12] and poplar plastocyanin[13] and their application to data analysis are described in earlier publications. $Cs_2CuCl_4$ crystallizes in the orthorhombic space group *Pnam*. There are four molecules per unit cell which form two pairs related by glide planes. Although the symmetry of the molecule is only $C_s$ from crystallographic symmetry, the anion has approximate $D_{2d}$ symmetry. The molecular axes are defined such that the *z* axis is perpendicular to the plane that the $CuCl_4^{2-}$ anion would occupy if it were flattened to $D_{4h}$ symmetry. The molecular *x* and *y* axes are defined along the projections of the Cu–Cl bonds in the hypothetical flattened plane.[25] One of the *xy* axes (arbitrarily chosen as *y*) is aligned parallel to the crystallographic *c* axis. Due to the space group symmetry, the two distinct molecular *x* axes (and the molecular *z* axes) are separated by 75°. The observed transition strengths along each crystallographic axis $I_a$, $I_b$, and $I_c$ are then:

$$I_a = 0.63I_x + 0.37I_z$$

$$I_b = 0.37I_x + 0.63I_z$$

$$I_c = I_y$$

where $I_x$, $I_y$, and $I_z$ are the molecular absorption cross sections. Data were measured along each crystallographic axis, and from these data it is possible to determine the isolated molecular transition strengths.

**E. Fitting Procedures.** Data were fit with the nonlinear least-squares fitting program FITCUR. FITCUR was written by Dr. Geoffrey S. Waldo, now at North Carolina State University, then in the laboratory of Prof. James E. Penner-Hahn. The program was modified at Stanford University by Dr. Soichi Wakatsuki to include the option of imposing separate optimization weightings for the fit to the data, the first derivative, and/or the second derivative of the data. In the fitting experiments described herein, the weighting scheme used for the fits was the following: data, 0.70; first derivative, 0.0; second derivative, 0.30. Pre-edge features were modeled by Lorentzian or Gaussian functions. Neither function by itself is completely adequate for fitting the pre-edge features, as the features are expected to be a convolution of the Lorentzian transition envelope[26] and the Gaussian imposed by the spectrometer optics.[27] Functions were chosen which were found empirically to give the best fit. The rising edge was modeled by either an arctangent function or the tail of a Lorentzian function. For spectra consisting of a pre-edge feature and a smooth rising edge, one function for the rising edge and one function for the pre-edge feature were all that was necessary, and a best fit minimum was found fairly easily.

For edges with a complicated line shape, such as the *z*-polarized Cu K-edge spectrum of $Cs_2CuCl_4$, the following approach was taken. The number and positions of the functions used were chosen on the basis of the features evident in the second derivative of the spectrum. Functions for fitting were chosen on the basis of the criteria that the features of both the data and of the second derivative should be reproduced. It was found that for this fit the feature at ~8987 eV was best modeled using a combination of Lorenztian and Gaussian contributions. All parameters (maximum height, FWHM, and energy position) of each feature were allowed to vary, with the exception of those parameters which varied to unreasonable values (e.g., a FWHM which varied to over 4.8 eV). These parameters' values were fixed for each fit and systematically stepped through a series of reasonable values. Fits were examined carefully and the best value for the parameter, based on the above criteria, was chosen. In some cases, the goodness-of-fit was invariant to the value of the fixed parameter and a series of equivalently good fits resulted. The standard deviation of the fit (as calculated by FITCUR) was the same for a series of equivalently good fits. Areas for fitted features were approximated by the maximum height *x* FWHM. It was found that this approximation gave within error the same results as an analysis which utilized the actual integrated intensities. The reported intensity ratios between features modeled in the fit is the average ratio for the series of equivalently good fits; the error is the standard deviation.

**F. Error Analysis.** There are several possible sources of systematic error in this analysis. Normalization procedures can introduce a 1–3% difference in pre-edge peak heights as determined by varying the parameters used to normalize a set of Cl K-edge spectra, while still requiring the final fits to meet requirements of consistency. This ~3% error is reported for peak heights when comparisons between two sets of data are being made. However, for comparison of intensities of several features in a given spectrum, the difference has been scaled for all features and normalization does not introduce significant variation in the ratios between features. Further, the choice of functions/parameters used to fit spectra can also introduce errors. Estimation of this error requires comparing fits to the data which use a variety of functions and parameters defining those functions. In our analysis of the fitting of *z*-polarized Cu K-edge of $D_{2d}$ $CuCl_4^{2-}$, we found that while the absolute variation in the intensities of given features was large (up to ~8%), the variation in the range of ratios between features was much less. Comparison of all reasonable fits showed a range of less than 1%, while inclusion of less-

(25) In this molecule the $3d_{xy}$ ground state is equivalent to the $3d_{x^2-y^2}$ ground state of $D_{4h}$ $CuCl_4^{2-}$ as a result of a 45° rotation of the *xy* molecular coordinate system and will be referred to herein as a $3d_{x^2-y^2}$ ground state.

(26) Agarwal, B. K. *X-ray Spectroscopy*; Springer-Verlag: Berlin. 1979; p 276ff.

(27) (a) Tyson, T. A.; Roe, A. L.; Frank, P.; Hodgson, K. O.; Hedman, B. *Phys. Rev. B* **1989**, *39A*, 6305–6315. (b) Lytle, F. W. In *Applications of Synchrotron Radiation*; Winick, H., Xian, D., Ye, M. H., Huang, T. Eds.; Gordon and Breach: New York, 1989; p 135. (c) Lytle, F. W.; Greegor, R. B.; Sandstrom, D. R.; Marques, E. C.; Wong, J.; Spiro, C. L.; Huffman, G. P.; Huggins, F. E. *Nucl. Instr. Meth.* **1984**, *226*, 542–548.

Table II. Input Parameters for Cu-tet *b* SCF-X$\alpha$-SW Calculation

| atom | position[a] x | y | z | sphere radius | $\alpha$ value | $l_{max}$ |
|---|---|---|---|---|---|---|
| out | 0.0000 | 0.0000 | 0.0000 | 9.35 | 0.736 63 | 4 |
| Cu | 0.0000 | 0.0000 | 0.0000 | 2.95 | 0.706 97 | 3 |
| S | 4.5213 | 0.0000 | 0.0000 | 2.50 | 0.724 75 | 2 |
| N1 | -0.134 11 | 0.0000 | 3.8316 | 1.90 | 0.751 97 | 2 |
| H | 0.790 00 | -1.6427 | 4.5346 | 1.17 | 0.777 25 | 0 |
| H | 0.790 00 | 1.6427 | 4.5346 | 1.17 | 0.777 25 | 0 |
| H | -2.0528 | 0.0000 | 4.4360 | 1.17 | 0.777 25 | 0 |
| N2 | -0.134 11 | 0.0000 | -3.8316 | 1.90 | 0.751 97 | 2 |
| H | 0.790 00 | 1.6427 | -4.5346 | 1.17 | 0.777 25 | 0 |
| H | 0.790 00 | -1.6427 | -4.5346 | 1.17 | 0.777 25 | 0 |
| H | -2.0528 | 0.0000 | -4.4360 | 1.17 | 0.777 25 | 0 |
| N3 | -2.5480 | 3.2568 | 0.0000 | 1.90 | 0.751 97 | 2 |
| H | -2.2141 | 4.3690 | 1.6426 | 1.17 | 0.777 25 | 0 |
| H | -2.2141 | 4.3690 | -1.6426 | 1.17 | 0.777 25 | 0 |
| H | -4.4551 | 2.6170 | 0.0000 | 1.17 | 0.777 25 | 0 |
| N4 | -2.5480 | -3.2568 | 0.0000 | 1.90 | 0.751 97 | 2 |
| H | -2.2143 | -4.3689 | -1.6426 | 1.17 | 0.777 25 | 0 |
| H | -2.2143 | -4.3689 | 1.6426 | 1.17 | 0.777 25 | 0 |
| H | -4.4551 | -2.6170 | 0.0000 | 1.17 | 0.777 25 | 0 |
| C | 5.5807 | 0.0000 | -3.2607 | 1.80 | 0.759 28 | 2 |
| H | 4.8860 | -1.6426 | -4.1911 | 1.17 | 0.777 25 | 0 |
| H | 4.8860 | 1.6426 | -4.1911 | 1.17 | 0.777 25 | 0 |
| H | 7.5916 | 0.0000 | -3.3130 | 1.17 | 0.777 25 | 0 |

[a] Coordinates are in Bohr units.

good fits with different fitting functions only increased this range to 1.5%. This error is reported in the analysis. In less complicated spectra (e.g., the S K-edges described herein), the error introduced by fitting is minimal.

**G. SCF-X$\alpha$-SW Calculations.** Standard SCF-X$\alpha$-SW calculations on the Cu-tet *b* molecule were performed on DEC station 3100 computers with between 300 and 400 iterations required for convergence. The calculations were considered to have converged when the largest relative change in the potential between subsequent iterations was less than $10^{-4}$. Each nitrogen ligated to the copper was approximated by an amine group, and the thiolate group was modeled with methyl thiolate. The Cu-tet *b* calculation was performed with a 5-coordinate geometry having idealized $C_s$ symmetry. Distances and angles were averaged from the crystal structure values. The coordinate system was chosen to reproduce the experimentally observed $d_{x^2-y^2}$ ground state. The position of the atoms, sphere radii, $\alpha$ values, and maximum values for the azimuthal quantum number are given in Table II. Sphere radii used were the same as in our previous calculation on plastocyanin, which were chosen by fitting the calculation to the experimental *g* values.[2b] The $\alpha$ values were those determined by Schwartz,[28] while a Watson sphere coincident with the outer sphere radius was used in calculations of charged species. Optical transition energies were determined by using the Slater transition-state formalism.

## Results and Analysis

**(A) Cu K-Edge Spectroscopy. Cu 1s → 3d Quadrupole Transition Intensity.** Figure 2 shows the polarized Cu K-edge spectra of $D_{4h}$ $CuCl_4^{2-}$. Because the inversion symmetry of the anion rules out Cu 4p mixing into the ground-state orbital, the 1s → 3d pre-edge transition is not expected to have any electric dipole intensity. However, the spectra clearly show pre-edge transition intensity in the 8979-eV region. The maximum intensity is observed for the *xy* orientation (Figure 2a) for which $\phi = 45°$ and in which the half-occupied $3d_{x^2-y^2}$ orbital transforms as $d_{xy}$ in the coordinate frame of the incoming radiation; the molecule lies in the plane of the polarization and the polarization vector **E** bisects the Cl–Cu–Cl (90°) angles. We have shown previously that this ~8979-eV feature can be assigned as a 1s → 3d quadrupole transition.[12] At Cu K-edge energies (9000 eV) the X-ray photon wavelength ($\lambda$ = 1.38 Å) is not large relative to the orbital of the electron, and higher order terms in the transition moment multipole expansion become significant. The intensity of the *xy*-polarized 1s → 3d feature does not go to zero at the minimum of the quadrupole variation ($\phi = 0°$). A close examination of the crystal structure of this system shows that there are two $CuCl_4^{2-}$ molecules per unit cell whose *z* axes are equally displaced from the crystallographic *c* axis and whose *xy* planes are rotated ~15° from one another. This misalignment of the molecules accounts for ~22% of the residual intensity in the pre-edge feature. The experimental uncertainty in the crystal alignment (~5°) accounts for an additional ~10%, assuming the full 5° misalignment. The remaining intensity probably has its origin in vibronic coupling.[29]

The *z*-polarized spectrum of $D_{4h}$ $CuCl_4^{2-}$ in Figure 2b exhibits a weak pre-edge feature at ~8979 eV, the intensity of which is comparable to the minimum *xy*-polarized intensity at $\phi = 0°$. This feature has been observed by Kosugi and co-workers in a previous study of this complex.[30] The quadrupole transition will not contribute to pre-edge intensity in the *z*-polarized spectrum, so this weak feature must also originate from vibronic coupling. The most prominent feature in the *z*-polarized spectrum is a very intense feature at 8986.1 eV, which is absent in the *xy*-polarized spectrum. The intensity of the feature suggests that it is an allowed transition and is probably associated with the 1s → 4p transition. As will be described later in this paper, our previous Cu K-edge XAS study of copper(II) model complexes (including $D_{4h}$ $CuCl_4^{2-}$) assigned this feature as a Cu 1s → 4p transition with a simultaneous ligand-to-metal CT (LMCT) shakedown.[11] Based on results from ab initio calculations, Kosugi and co-workers also assigned this feature as a 1s → 4p + LMCT shakedown transition.[30]

The polarized Cu K-edge study of $D_{4h}$ $CuCl_4^{2-}$ shows that quadrupole intensity contributes to 1s → 3d transition intensity at ~8979 eV. For other copper(II) systems the quadrupole contribution to the 1s → 3d transition intensity will be similar to that in $D_{4h}$ $CuCl_4^{2-}$, assuming that the magnitude of the $3d_{x^2-y^2}$ orbital character in the ground-state wave function is similar. The quadrupole transition intensity is not isotropic; it will contribute in nonpolarized and *xy*-polarized spectra.

**Nonpolarized Cu 1s → 3d Intensity.** Nonpolarized Cu K-edge X-ray absorption spectra for $D_{4h}$ and $D_{2d}$ $CuCl_4^{2-}$ and for plastocyanin are given in Figure 3. All have a feature at ~8979 eV, which can be assigned as the 1s → 3d transition. The observed pre-edge intensity (Figure 3, inset) for the $D_{2d}$ complex is about 3 times as intense as in the $D_{4h}$ complex, while that of plastocyanin is about 2 times as intense as in the $D_{4h}$ complex. X$\alpha$ calculations[9] indicate that the $3d_{x^2-y^2}$ component of the ground state is similar for $D_{4h}$ and $D_{2d}$ $CuCl_4^{2-}$, being 61% and 67%, respectively. Thus, we can take the quadrupole intensity in the $D_{4h}$ spectrum as a base line for the feature in the spectrum of the $D_{2d}$ complex. X$\alpha$ calculations on the blue copper site[2] indicate that the ground state is only 42% $3d_{x^2-y^2}$. We would expect, then, that the contribution to the intensity from the quadrupole transition in plastocyanin will be less than in the $D_{4h}$ case. The source of the additional intensity in the $D_{2d}$ complex and plastocyanin must therefore be attributed to 4p mixing into the ground state.

**Cu 1s → 4p + LMCT Shakedown Transition: Quantitating Intensity.** The nature of the 4p mixing into the $3d_{x^2-y^2}$ ground state of $D_{2d}$ $CuCl_4^{2-}$ has been investigated with single crystal polarized experiments. Figure 4 shows the *y*- and *z*-polarized spectra of $D_{2d}$ $CuCl_4^{2-}$ (note that the *x*- and *y*-polarizations are equivalent in this system). The *y*-polarized spectrum exhibits no pre-edge feature, while the ~8979 eV pre-edge feature is present in the *z*-polarized spectrum. In the *y*-polarized orientation the half-occupied $3d_{x^2-y^2}$ orbital does not transform as $d_{xy}$ in the coordinate frame of the incoming radiation, so the quadrupole transition is not expected to be observed. There is also no *y*-polarized electric dipole intensity, ruling out $4p_{xy}$ mixing into the ground-state orbital. The *z*-polarized ~8979-eV feature must originate from $4p_z$ mixing into the ground state, as the quadrupole transition does not contribute to *z*-polarized spectra. Note that it is this $4p_z$ mixing which has been postulated to reduce the EPR parallel hyperfine splitting of this complex.

(28) Schwarz, K. *Phys. Rev. B* **1972**, *5*, 2466–2468.

(29) The effect of incomplete polarization of the beam cannot be quantitated for this data as it was not measured at the time of the experiment.

(30) Kosugi, N.; Yokoyama, T.; Asakura, K.; Kuroda, H. *Chem. Phys.* **1984**, *91*, 249–256.

Additionally, in the *z*-polarized spectrum, there is a well-resolved feature on the rising edge at ~8987 eV. This is comparable to the ~8986-eV feature in the *z*-polarized spectrum of $D_{4h}$ $CuCl_4^{2-}$ in Figure 2b. It is assigned as a Cu 1s → 4p + ligand-to-metal CT (LMCT) shakedown transition made allowed by final-state relaxation. Our previous study of a series of copper(II) compounds found that this feature appears between 8986 and 8988 eV in all complexes studied.[11a] In systems characterized by more covalent interactions with the ligands, the feature appears in the lower end of this energy range.[11a] The process of excitation of a 1s core electron into the 4p orbital (an electric dipole-allowed transition) creates a core hole, which results in an increased effective nuclear charge felt by the valence orbitals. This causes relaxation of the copper valence orbitals to deeper binding energies (Figure 5). The half-occupied $3d_{x^2-y^2}$ orbital relaxes to an energy below that of the ligand valence levels. As a result of this relaxation, a lower energy configuration is possible; an electron from the ligand valence is transferred to the copper and fills the $3d_{x^2-y^2}$ orbital. This excited configuration gives rise to a lower energy transition, observed as a feature on the rising edge. Covalency increases as the ligand ionization energy decreases; the ligand valence level comes closer in energy to the half-occupied Cu 3d orbital in the ground state. As the energy of the ligand 3p level increases, the stabilization of the 3d orbital upon core ionization *relative* to the ligand 3p orbital becomes greater. Thus, one would expect the energy of the shakedown transition to decrease as the covalency increases, which is the experimentally observed result. Further, a shakedown assignment is required in the interpretation of the Cu(II) 2p XPS spectrum,[9] and its extension to the 1s core absorption is reasonable and consistent with ab initio calculations.[10k,30]

The observed shakedown is analogous to the satellites observed in PES spectra and can be treated in a similar manner.[9] This treatment enables us to quantify the intensity of the 1s → 4p + LMCT shakedown feature as a percentage of the total 1s → 4p transition intensity. Comparison of the shakedown intensity to that of the 1s → 3d(+4p) transition (~8979 eV) then allows for quantitation of the amount of $4p_z$ mixing into the ground-state 3d orbital. In the sudden approximation,[31] the creation of the core hole occurs rapidly, before the remaining electrons adjust to the new potential. The intensity $I_i$ of a given transition i corresponding to either the main or shakedown final state can then be expressed as

$$I_i = |\langle \Psi_i(\underline{c}) | \Psi_R(\underline{c}) \rangle|^2$$

where $\underline{c}$ denotes a core hole, $\Psi_i$ denotes the relaxed final states (the main and the shakedown peaks), and $\Psi_R$ is the initial unrelaxed state with the core electron removed. This implies that only initial and final states with the same symmetry can contribute to shakedown intensity. Quantitation of this process and determination of the intensity ratio of the main peak to the shakedown peak can be obtained through the use of a configuration interaction type model. The ground-state wave function $\Psi_g$ for the $D_{2d}$ complex is obtained by diagonalizing the energy matrix

$$\begin{vmatrix} \langle \Psi(3d^9)|H|\Psi(3d^9)\rangle - E' & \langle \Psi(3d^9)|H|\Psi(3d^{10}\underline{L})\rangle \\ \langle \Psi(3d^9)|H|\Psi(3d^{10}\underline{L})\rangle & \langle \Psi(3d^{10}\underline{L})|H|\Psi(3d^{10}\underline{L})\rangle - E' \end{vmatrix}$$

where $\Psi(3d^9)$ and $\Psi(3d^{10}\underline{L})$ represent the one-hole metal state and the $d^{10}$ metal/one-hole ligand state, respectively. Diagonalization gives the eigenvector corresponding to the lowest energy state as eq 2,

$$\Psi_g = \cos\theta|3d^9\rangle - \sin\theta\,|3d^{10}\underline{L}\rangle \quad (2)$$

with $\tan 2\theta = 2T/\Delta$, $T = \langle \Psi(3d^9)|H|\Psi(3d^{10}\underline{L})\rangle$, and $\Delta = \langle \Psi(3d^9)|H|\Psi(3d^9)\rangle - \langle \Psi(3d^{10}\underline{L})|H|\Psi(3d^{10}\underline{L})\rangle$. $T$ is the interaction matrix element between the configurations contributing to the ground-state wave function, and $\Delta$ is the energy difference between the two configurations, as shown in Figure 6a.

The 1s → 4p transition and corresponding creation of the core hole produce two possible final states corresponding to a main ($\Psi_m$) and a shakedown ($\Psi_s$) peak. The interaction matrix for the excited states is constructed in an analogous fashion as for the ground state, with the addition of a term ($Q$) to the diagonal energy of the $\underline{c}3d^9$ configuration to account for the increase in the effective nuclear charge felt by the $3d^9$ state (Figure 6b). The solutions for the excited-states wave functions are given by eqs 3a and b, where $\underline{c}$ indicates a Cu 1s core hole and $\tan 2\theta' = 2T/(\Delta - Q)$; $0 < \theta' < 90°$.

$$\Psi_m = \sin\theta'|\underline{c}3d^9\rangle + \cos\theta'|\underline{c}3d^{10}\underline{L}\rangle \quad (3a)$$

$$\Psi_s = \cos\theta'|\underline{c}3d^9\rangle - \sin\theta'|\underline{c}3d^{10}\underline{L}\rangle \quad (3b)$$

The energy splitting $W$ between the main and shakedown peaks is given by eq 4.

$$W = [(\Delta - Q)^2 + 4T^2]^{1/2} \quad (4)$$

The main-to-shakedown peak intensity ratio ($I_m/I_s$) is given by eq 5.

$$\frac{I_m}{I_s} = \left(\frac{\sin\theta'\cos\theta - \cos\theta'\sin\theta}{\cos\theta'\cos\theta + \sin\theta'\sin\theta}\right)^2 = \tan^2(\theta' - \theta) \quad (5)$$

Thus, the intensity ratio is determined by the change in the wave function $\theta' - \theta$ upon the creation of a 1s core hole. PES satellite features have already provided an analysis of $CuCl_4^{2-}$ complexes for ionization of a 2p core electron.[9] The PES study found that $\Delta = 0.88$ eV, $T = 1.5$ eV, $Q = 8.9$ eV, and $W = 8.20$ eV for the $D_{2d}$ $CuCl_4^{2-}$ complex. Because $\Delta$ and $T$ are ground-state parameters, the values determined in the PES study can be used in the analysis of the XAS shakedown intensity in $D_{2d}$ $CuCl_4^{2-}$. The value of $Q$ for the 1s → 4p promotion is not known. As a first approximation, the relaxation $Q$ is assumed to be the same as for the 2p ionization. Our analysis, then, takes the following approach: (i) use ground-state values for $CuCl_4^{2-}$ as determined by PES; (ii) assume $W = 8.20$ eV as a first approximation for the energy splitting between the main and shakedown features; and (iii) fit the data to quantitate intensities and to obtain experimental energy splittings.

The fitting procedures showed that a feature could not reasonably be fit at 8.20 eV above the shakedown feature energy. However, the fit consistently required a feature 6.6 eV above the shakedown feature. We thus assign the feature at 8993.1 eV in the *z*-polarized spectrum in Figure 4 as the 1s → 4p main transition. The observed energy splitting relative to the shakedown peak ($W = 6.6$ eV) was used to calculate the relaxation in the system to find that $Q = 6.8$ eV. This relaxation is less than that of a 2p ionization because the promoted electron is in a bound valence state, reducing the effective nuclear charge felt by the valence orbitals.

Using this adjusted value of $Q$, the $I_m/I_s$ intensity ratio is calculated to be 0.69. Thus the main transition contains 41% of the 1s → 4p transition intensity and the shakedown transition contains 59%. The fitting procedure gave a $I_m$:$I_s$ ratio of ~60:40. However, the fitted intensity of the main transition $I_m$ is complicated by the rising-edge background. This fit to both the data and to the second derivative of the data for the *z*-polarized $D_{2d}$ XAS spectrum is shown in Figure 7. An examination of the resultant equivalently good fits (Table I) shows that the ratios between features in the fitted spectrum are relatively constant, despite small changes in the absolute areas of the features. Further, the ratio between the areas of the ~8979 eV (1s → 3d(+4p)) transition and the ~8987 eV shakedown feature is found to be

$$\frac{I(\sim 8979)}{I(\sim 8987)} = 0.0636 \pm 0.0005$$

The 4p mixing into the $3d_{x^2-y^2}$ ground state can now be determined because the intensity of the transition will be proportional to the

(31) (a) Manne, R.; Åberg, T. *Chem. Phys. Lett.* **1970**, *7*, 282–284. (b) Larsson, S. *Phys. Scr.* **1977**, *16*, 378–380. (c) van der Laan, G.; Westra, C.; Haas, C.; Sawatzky, G. A. *Phys. Rev. B: Condens. Matter* **1981**, *23*, 4369–4380.

amount of electric dipole transition character in that transition integral. Quadrupole contribution to the intensity of the ~8979 eV feature need not be considered because it is not allowed for the z-polarization. As calculated from the intensity ratio $I_m/I_s$ the shakedown feature reflects 59% of the pure 1s → 4p transition. The 1s → 3d(+4p) transition must then reflect 3.8 ± 1.5% 4p character. Thus, there is ~4% $4p_z$ mixing into the ground state of $D_{2d}$ $CuCl_4^{2-}$. This result is consistent with Xα calculations on this site.[9] As in the $D_{4h}$ $CuCl_4^{2-}$ complex, vibronic coupling may contribute to the intensity of the ~8979 eV feature in this system. Thus, the 3.8% 4p mixing from the above analysis reflects an upper limit of the magnitude of direct 4p mixing in the half-occupied orbital of this complex.

The results of this shakedown analysis are inconsistent with the requirement that there be 12% $4p_z$ mixing in the ground state of $D_{2d}$ $CuCl_4^{2-}$ to reproduce the observed small hyperfine splitting in the EPR spectra. An alternative explanation for the small EPR parallel hyperfine must therefore be considered.

**Cu 1s → 3d Transition in Plastocyanin: Probing Cu 4p-Mixing.** Polarized single crystal XAS studies at the Cu K-edge of plastocyanin allow us to probe Cu 4p mixing into the active-site ground state. Figure 8 presents polarized X-ray absorption spectra of oriented plastocyanin crystals, previously published in ref 13. A pre-edge feature at ~8979 eV, assigned as the 1s → 3d(+4p) transition, is maximized in the xy-polarized spectrum and absent in the z-polarized spectrum. Because the orientation which gives rise to the spectrum in Figure 8b places the xy plane perpendicular to the propagation of light, it exhibits no quadrupole intensity. The nonpolarized Cu K-edge data (Figure 3c) show that the plastocyanin 1s → 3d transition has electric dipole intensity which is attributed to 4p mixing into the ground-state wave function. The data in Figure 8 clearly show that the 1s → 3d(+4p) electric dipole transition is xy polarized; thus it must be $4p_{xy}$ mixing which accounts for the observed intensity. The electric dipole intensity in this feature varies as $\cos^2\phi$ and is maximized ($\phi = 0°$) when the polarization vector is coincident with the p orbital which is allowed by group theory to mix with the $3d_{x^2-y^2}$ orbital.[32] The four molecules in the plastocyanin unit cell are aligned such that the p orbitals responsible for electric dipole intensity are oriented in two sets at 90° to each other. Thus, in contrast to the previous interpretation of these data,[13] the electric dipole intensity is isotropic with respect to the xy plane of the plastocyanin crystal system (data not shown). Note that both the effective $C_{3v}$ symmetry determined by ligand field analysis and the Xα calculations predicted this $p_{xy}$ mixing into the plastocyanin ground state.

The absence of any 1s → 3d pre-edge intensity in the z-polarized spectrum rules out the possibility of $p_z$ mixing in the ground-state wave function of the blue copper site. Thus, 12% $4p_z$ mixing into the Cu $3d_{x^2-y^2}$ ground state cannot be the explanation for the observed small hyperfine splitting in the EPR spectra of the blue copper proteins.

**(B) Ligand K-Edge Spectroscopy. Cl K-Edge Spectroscopy.** It is clear from the Cu K-edge studies that the origin of the small $A_\parallel$ splitting in the EPR spectra of $D_{2d}$ $CuCl_4^{2-}$ and blue copper centers is not $4p_z$ mixing. The alternative explanation for the reduced hyperfine splitting, high covalency, has therefore been explored experimentally. An estimate of the covalency of a metal–ligand bond can be obtained from ligand K-edge studies. Our previous study shows that the Cl K-edge spectra of $D_{4h}$ and $D_{2d}$ $CuCl_4^{2-}$ exhibit a well-resolved, intense pre-edge feature at ~2820 eV.[16] As discussed in the introduction (eq 1), the intensity of the transition is proportional to the covalent mixing of the Cu $3d_{x^2-y^2}$ with the four chloride ligands due to bonding.

Figure 9, which presents higher resolution data than ref 16, shows that the pre-edge feature in $D_{2d}$ $CuCl_4^{2-}$ is less intense than in $D_{4h}$ symmetry and that the feature in the $D_{2d}$ spectrum lies at

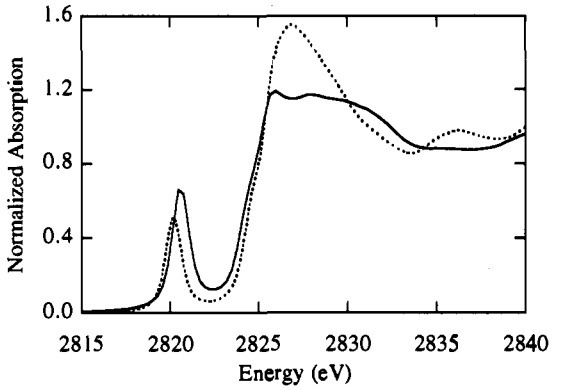


**Figure 9.** Cl K-edge spectra of $D_{4h}$ $CuCl_4^{2-}$ (—) and $D_{2d}$ $CuCl_4^{2-}$ (---). The pre-edge feature at ~2820 eV is assigned as a Cl 1s → ψ* transition, where ψ* is an antibonding molecular orbital with both Cl 3p character and Cu $3d_{x^2-y^2}$ character. The intensity reflects the magnitude of the electric dipole-allowed component of the transition (Cl 3p) and therefore reflects the covalent contribution of the ligand to ψ*.

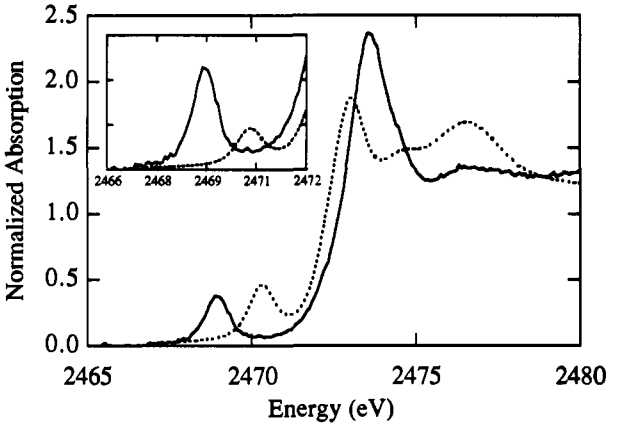


**Figure 10.** S K-edge spectra of the blue copper model Cu-tet *b* (---) and spinach plastocyanin (—). The inset shows the pre-edge regions of the spectra only, with the plastocyanin data rescaled by a factor of 3 (see text). The intensity of the pre-edge feature reflects the covalent contribution of the thiolate ligand to the ground-state molecular orbital.

0.4 eV lower energy. Analysis of EPR superhyperfine splitting in $D_{4h}$ $CuCl_4^{2-}$ has established that its ground-state orbital is best described as 61% Cu $3d_{x^2-y^2}$ and 39% Cl 3p.[33] If $\alpha'^2 = 0.39$ for $D_{4h}$, one can compare the experimental pre-edge intensities to determine that $\alpha'^2 = 0.29$ for $D_{2d}$ $CuCl_4^{2-}$. Thus, the ground-state orbital in $D_{2d}$ $CuCl_4^{2-}$ is ~71% Cu $3d_{x^2-y^2}$ and ~29% Cl 3p, in good agreement with Xα calculations which predict 67% $3d_{x^2-y^2}$ in the ground state.[9] Thus, the Cl K-edge data show that the small EPR $A_\parallel$ hyperfine in the $D_{2d}$ site also cannot be explained by a high degree of $3d_{x^2-y^2}$ covalency for the site. The origin of this splitting is addressed in the Discussion section of this paper.

The 0.4-eV energy difference in the pre-edge transitions can be understood in terms of relative repulsion of the $3d_{x^2-y^2}$ orbital due to differences in ligand field strength. The $D_{4h}$ $3d_{x^2-y^2}$ orbital lobes are directed along the Cu–Cl bonds and therefore experience more repulsion than in the $D_{2d}$ geometry in which the Cu–Cl bonds are distorted away from the xy plane. Thus, the transition to the orbital containing $3d_{x^2-y^2}$ character occurs at higher energy in $D_{4h}$ $CuCl_4^{2-}$. This is in quantitative agreement with configuration interaction calculations for PES spectra on these sites, which predict a ~0.5 eV increase in the $3d_{x^2-y^2}$ orbital energy in the $D_{4h}$ ligand field.[9]

**S K-Edge Spectroscopy.** Sulfur K-edge data of the thiolate model complex, Cu-tet *b*, and plastocyanin are shown in Figure 10. Both spectra have an intense, well-resolved pre-edge feature at ~2470 eV assigned as a S(thiolate) 1s → ψ* transition, where ψ* is the molecular orbital containing Cu $3d_{x^2-y^2}$ and S(thiolate)

(32) If the coordinate system of the plastocyanin molecule is rotated about z by 45° to define axes x′ and y′ (for the purpose of analysis), the ground-state orbital is $d_{x'y'}$ and the Cu–S(Cys) bond is along the x′ axis. In $C_s$ symmetry it is found[2] that only the $p_{y'}$ orbital mixes with the ground-state orbital. In the orientation which gives rise to Figure 8b, each $p_{y'}$ orbital is oriented 45° from E.

(33) Solomon, E. I. *Comments Inorg. Chem.* **1984**, *3*, 297–299.

**Table III.** Results of SCF-Xα-SW Calculation for the Highest Occupied Valence Levels of Cu-tet *b*: Ground-State Orbital Energies and Charge Distribution

| level | energy (eV) | character[a] |
|---|---|---|
| 18a′ | −2.467 | 66% Cu[0.88$d_{x^2-y^2}$ + 0.11$d_{z^2}$] (ab) 15% $Sp_\sigma$ + ~20% N |
| 10a″ | −3.169 | 35% Cu[0.88$d_{xz}$] (ab) 51% $Sp_\pi$ + ~12% N |
| 17a′ | −3.806 | 68% Cu[$d_{z^2}$] (ab) 21% $Sp_\sigma$ + ~12% N |
| 9a″ | −4.205 | 53% Cu[$d_{xz}$] (b) 32% $Sp_\pi$ + ~18% N |
| 16a′ | −4.431 | 94% Cu[$d_{xy}$] (nb) 3% Sp |
| 8a″ | −4.459 | 98% Cu [$d_{yz}$] |
| 15a′ | −5.074 | 55% Cu [0.47$d_{x^2-y^2}$ + 0.41 $d_{z^2}$ + 0.11 $d_{xy}$] (b) 37% $Sp_\sigma$ |

[a] (ab) denotes antibonding interaction; (b) denotes bonding interaction; (nb) denotes a nonbonding state.

3p orbital character. In both spectra the data are normalized to an edge jump of one sulfur. Plastocyanin has a total of three sulfur atoms, but only the cysteine sulfur ligand has overlap with the Cu $3d_{x^2-y^2}$ orbital and contributes to pre-edge intensity. (One of the sulfur residues is not ligated to the copper. From single crystal EPR it is known that the methionine sulfur ligand bond is perpendicular to the half-occupied orbital and has no net overlap with this orbital.[8] Xα calculations[2a] have further verified that there is no S(Met) character in the half-occupied orbital. Note that the S(Met) does undergo a bonding interaction with the fully-occupied $d_{z^2}$ orbital.) To compare pre-edge intensities the plastocyanin spectrum must thus be renormalized by a factor of 3 (Figure 10, inset). The pre-edge intensity of plastocyanin is much greater than that of Cu-tet *b*. Both the Cu-tet *b* and plastocyanin renormalized pre-edge regions were fit as described in the Experimental Section; the Cu-tet *b* pre-edge intensity (approximated by the height x FWHM) is 0.38, while the plastocyanin intensity is 0.97. Because the pre-edge intensity is a direct probe of the covalency of the Cu–S bond, these data clearly show that, relative to the Cu-tet *b* complex, plastocyanin has a highly covalent Cu–S(Cys) bond.

In order to interpret the covalency reflected in the S K-edge pre-edge intensities in a more quantitative fashion, it is important to have an understanding of the electronic structure of the Cu-tet *b* model complex and its relation to the electronic structure of plastocyanin. To this end, we have performed Xα calculations on Cu-tet *b*, the parameters for which are given in Table II. The highest occupied valence molecular orbitals for the Cu-tet *b* molecule are shown in Table III. The metal contribution to the ground-state wave function (state 18a′) is 0.88 $d_{x^2-y^2}$ and 0.11 $d_{z^2}$. These contributions help to picture the effective symmetry of this site. 5-Coordinate sites can be described as structural distortions along a $C_s$ distortion pathway between the two high-symmetry limits of square pyramidal and trigonal bipyramidal, where the square pyramidal has a $d_{x^2-y^2}$ ground state and the trigonal bipyramidal has a $d_{z^2}$ ground state. In the tetragonal coordinate system the trigonal bipyramidal ground state is written as 75% $d_{x^2-y^2}$ and 25% $d_{z^2}$.[34] Therefore, the 11% $d_{z^2}$ component of the ground state in Cu-tet *b* indicates a structure halfway between the two high-symmetry limits (Figure 11).

The calculation provides important insight into the character of the half-occupied molecular orbital. In contrast to the bonding scheme in plastocyanin in which the highest occupied molecular orbital (HOMO) contains a strong Cu $3d_{x^2-y^2}$–$Sp\pi$ antibonding interaction, the half-occupied orbital in Cu-tet *b* is rotated by 45° with respect the Cu–S(thiolate) bond and is characterized by a σ-antibonding interaction (Figure 12). It is much less covalent than plastocyanin, consisting of 66% Cu $3d_{x^2-y^2}/d_{z^2}$ and 15% Spσ, while the wave function in plastocyanin is 42% Cu $3d_{x^2-y^2}$ and 36% Spπ.[2] This difference in bonding is attributed to the increased Cu–S bond length of Cu-tet *b* (2.36 Å) relative to plastocyanin (2.13 Å), which reduces the π-interaction. The Cu–thiolate

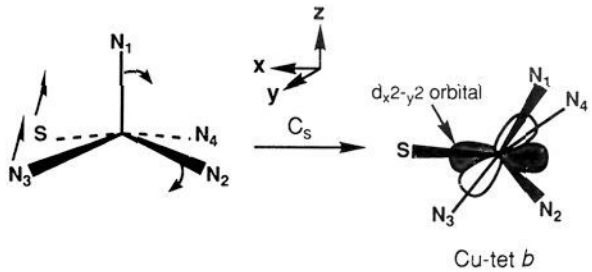


**Figure 11.** Schematic representation of the $C_s$ structural distortion from the 5-coordinate square pyramidal limit to the Cu-tet *b* molecular structure.

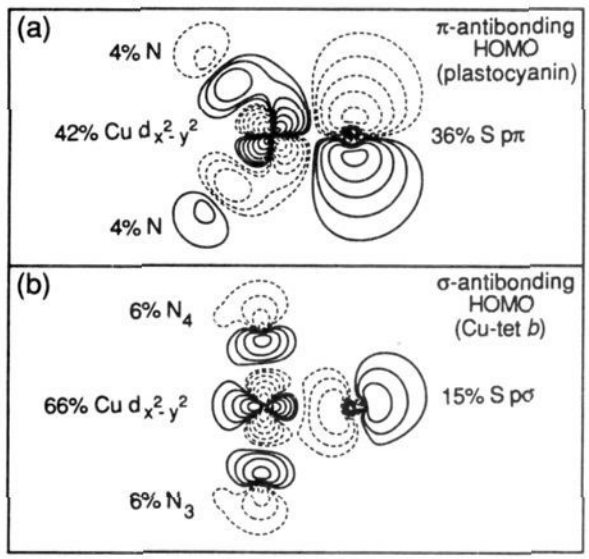


**Figure 12.** (a) Xα calculation contour plot of the highest occupied molecular orbital (HOMO) of plastocyanin showing the strong Cu–S(thiolate) π-interaction (taken from ref 2). (b) Xα calculation contour plot of the HOMO of Cu-tet *b* (state 18a′) showing the Cu–S(thiolate) σ-interaction. The $N_3$ and $N_4$ labels refer to the atom numbering shown in Figure 11. Note that, as described in Table III, the 66% Cu d-orbital character of this orbital is comprised of 88% $d_{x^2-y^2}$ and 11% $d_{z^2}$.

bonding in the Cu-tet *b* model complex is now understood, and the results of the calculation can be used to give a quantitative description of the S K-edge data. Thus, the pre-edge intensity of the S K-edge spectrum reflects a ~15% Sp contribution to the half-occupied ground-state orbital ($\alpha'^2 = 0.15$ for Cu-tet *b*). Using the protocol outlined in ref 16 and the quantitative intensities derived from the fits to the data, we find that the plastocyanin pre-edge intensity reflects 38% Sp character in the ground-state orbital. This is in quantitative agreement with the Xα calculation on plastocyanin, which gives the Sp contribution to the ground-state wave function to be 36%.[2] It is thus experimentally confirmed that the ground state of plastocyanin contains ~38 ± 3% Sp character. Further, we now have a quantitative description of sulfur pre-edge intensities with respect to covalency.

Having achieved a good description of the bonding in Cu-tet *b*, it is useful to relate this calculation to previously published spectral data.[17] Slater transition-state calculations were performed on selected states for comparison to the experimental absorption spectrum. The experimental charge-transfer (CT) bands appear[17] at ~23 500 and 27 800 $cm^{-1}$ for the Sπ- and Sσ-to-Cu CT transitions, respectively. The calculated transition energy for the Sσ CT transition (from state 15a′) is 26 762 $cm^{-1}$, in good agreement with experiment. The calculated transition energy for the Sπ CT transition (from state 9a″) is 15 365 $cm^{-1}$. This calculation gives an anomalously low result because states 8a″ and 9a″ come close in energy, resulting in a great deal of mixing of the two states and change in character of the wave functions upon ionization within the transition state. However, the calculations do predict the proper ordering of the Sσ and Sπ CT

(34) Wilcox, D. E.; Porras, A. G.; Hwang, Y. T.; Lerch, K.; Winkler, M. E.; Solomon, E. I. *J. Am. Chem. Soc.* **1985**, *107*, 4015–4027.

transitions. The experimental ligand field transitions[17] appear at 10 900, 13 700, and 17 000 $cm^{-1}$, with the 13 700 $cm^{-1}$ feature having an unusually high $\epsilon$ value for a d → d transition. The ligand field transition energies from states 17a′, 16a′, and 8a″ are calculated to be 11 130 ($d_{z^2}$), 17 446 ($d_{xy}$), and 18 389 $cm^{-1}$ ($d_{yz}$), respectively. Of the three ligand field transitions, only the 17a′ state ($d_{z^2}$) contains significant Sp ligand character due to configurational interaction with the 15a′ Sp$\sigma$ level. Thus, the most intense ligand field band at 13 700 $cm^{-1}$ is reasonably correlated with this transition.

The S K-edge data in Figure 10 also show that the pre-edge feature of Cu-tet *b* is higher in energy than in plastocyanin. The pre-edge feature in the Cu-tet *b* spectrum appears at 2470.3 eV, while that for plastocyanin is at 2469.0 eV. A comparison of the S K-edge pre-edge energies to the energies of the CT bands in the optical spectra (S$\pi$ CT in plastocyanin[2] and S$\sigma$ CT in Cu-tet *b*[17]) shows that there is a shift in the CT band to higher energy (relative to plastocyanin) in the Cu-tet *b* by 1.40 eV. Both the CT band and the S pre-edge feature reflect transitions to the $3d_{x^2-y^2}$ orbital. Clearly the distorted 5-coordinate geometry of Cu-tet *b* results in increased repulsion of the $3d_{x^2-y^2}$ orbital relative to that in plastocyanin, causing both the CT transition and the S K-edge pre-edge transition to occur at higher energy in the Cu-tet *b* spectrum. This is in agreement with X$\alpha$ calculations which indicate that the HOMO orbital is higher in energy in Cu-tet *b* than in plastocyanin by 0.7 eV.[2]

## Discussion

From single crystal polarized Cu K-edge XAS studies, it has been demonstrated that the origin of the small hyperfine splitting in blue copper centers is not 12% $4p_z$ mixing in the ground state. Further, the S K-edge data, in combination with X$\alpha$ calculations on the Cu-tet *b* model complex, show experimentally that the blue copper site is highly delocalized and is characterized by an unusually covalent Cu–S(Cys) bond. These results are in quantitative agreement with the X$\alpha$ calculation on the plastocyanin site, which indicates that the thiolate contribution to the ground-state wave function is ~38%.[2] It is now experimentally confirmed that delocalization of electron density onto the thiolate cysteine ligand is the origin of the small parallel hyperfine splitting in the EPR spectra of blue copper centers.

X$\alpha$ calculations on the Cu-tet *b* molecule have provided insight into Cu–S(thiolate) bonding in this complex. We have shown that the electronic structure of Cu-tet *b* is consistent with a geometry about halfway between the square pyramidal and trigonal bipyramidal limits. We have identified that the dominant bonding interaction in Cu-tet *b* is a Cu–S $\sigma$-interaction (in contrast to the $\pi$-interaction in blue copper), which is probably due to the increased bond length relative to that in the blue copper centers.

The origin of the small $A_\parallel$ hyperfine splitting in $D_{2d}$ $CuCl_4^{2-}$ can now be addressed. The Cu K-edge studies and shakedown transition analysis of $D_{2d}$ $CuCl_4^{2-}$ show that the magnitude of $4p_z$ mixing into the ground state is ~4%. Thus, as in blue copper, 12% $4p_z$ mixing can be ruled out as the origin of the small hyperfine splitting. In contrast to blue copper, Cl K-edges show that the complex is not unusually covalent. Therefore, the origin of the small hyperfine must be attributed to a large orbital dipolar contribution for which the sign is opposite that of the spin dipolar term associated with the half-occupied $3d_{x^2-y^2}$ orbital. This is consistent with our earlier studies of this complex.[9]

The contributions to the 1s → 3d transition intensity in the Cu K-edge at ~8979 eV are now well understood. Because higher order terms in the multipole expansion cannot be neglected at Cu K-edge energies, there is a contribution to the transition intensity from a 1s → 3d quadrupole-allowed transition. Additionally, in appropriate site symmetries 4p mixing into the $3d_{x^2-y^2}$ orbital gives electric dipole-allowed character to the transition. Polarized single crystal experiments are a useful probe into the nature and relative magnitude of this 4p mixing in a metal center. The transition in the Cu K-edge spectrum of Cu(II) complexes at ~8987 eV has been assigned as a 1s → 4p + LMCT shakedown transition. We have presented the first quantitative analysis of the intensity of this feature in Cu K-edge spectra and have assigned the 1s → 4p main transition in the *z*-polarized Cu K-edge spectrum of $D_{2d}$ $CuCl_4^{2-}$ at 6.6 eV higher energy. From this analysis, the energy and intensity of the shakedown pre-edge feature are related to the degree of relaxation which occurs upon promotion of the 1s electron to a valence orbital. We have observed experimentally that this relaxation is somewhat less than that for complete 2p ionization.

Ligand K-edge data have been shown to be a powerful tool in the study of the electronic structures of metal–ligand interactions in open shell metal ions. Ligand pre-edge intensity is a direct probe of the covalency of a metal–ligand bond, and the energies of ligand pre-edge transitions reflect the relative ligand field strength experienced by the metal in a given system. Ligand K-edges have a distinct advantage as a probe into the relative repulsion of a metal d-orbital in a ligand field due to the increased resolution of transitions in the soft X-ray region and the increased electric dipole-allowed intensity of ligand pre-edge features relative to pre-edge features at the metal K-edge. Ligand K-edges also have a strong advantage over traditional superhyperfine analysis of covalency in EPR spectroscopy since the ligand need not have a nuclear spin. In this paper, we have quantified the sulfur pre-edge intensity in terms of the covalency of the Cu–S bond using X$\alpha$ calculations and have thus presented the first use of ligand edges to quantitatively probe covalency in a metalloprotein.

**Acknowledgment.** This work was supported by grants from NSF (CHE91-21576, K.O.H.), (CHE89-19687, E.I.S.) and NIH (RR01209, K.O.H.). The data reported herein were collected at the Stanford Synchrotron Radiation Laboratory, which is supported by the U.S. Department of Energy, Office of Basic Energy Sciences, Divisions of Chemical Sciences and Material Sciences. The Stanford Synchrotron Radiation Laboratory is also supported in part by the National Institutes of Health, Biomedical Resource Technology Program, Division of Research Resources (RR-01209) and by DOE's Office of Health and Environmental Research (OHER). We also wish to thank Professor Hans C. Freeman of the University of Sydney who provided the poplar plastocyanin crystals and participated in the single crystal experiments for which the data was previously published in ref 13. We also thank Drs. Robert A. Scott and Teresa A. Smith who contributed to some of the early phases of this work.